

- 15, 1339.
- T. S. Lin and M. C. Liu, *Tetrahedron Lett.*, 1984, **25**, 905.
  - U. Niedballa and H. Vorbruggen, *J. Org. Chem.*, **39**, 3654 (1974).
  - Y. H. Kim, L. A. Pavelka, H. S. Mosher, F. A. Fuhrman, and G. J. Fuhrman, *Science*, **207**, 1935 (1980); Y. H. Kim, R. Nachman, L. Pavelka, H. S. Mosher, F. A. Fuhrman, G. J. Fuhrman, *J. Natural Products*, **44**, 206 (1981).
  - Unpublished data.
  - E. Wittenburg, *Angew. Chem.*, 1965, **77**, 1043.
  - J. C. Martin, C. A. Jeffery, D. P. C. Mieschael, M. A. Tipple, D. F. Smee, T. R. Matthews, and J. P. H. Verheyden, *J. Med. Chem.*, 1985, **28**, 358.

## Interaction of Metal Ions with NADH Model Compounds. Cupric Ion Oxidation of Dihyronicotinamides

Joon Woo Park\*, Sung Hoe Yun, and Kwanghee Koh Park†

Department of Chemistry, Ewha Womans University, Seoul 120-750

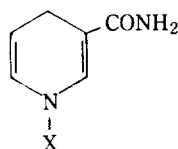
†Department of Chemistry, Chungnam National University, Daejeon 302-764. Received April 8, 1988

Kinetic studies on cupric ion ( $\text{Cu}^{2+}$ ) oxidation of 1-benzyl- and 1-aryl-1,4-dihyronicotinamides (XNAH) in aqueous solution were performed. In the presence of dioxygen ( $\text{O}_2$ ), the reaction followed first order kinetics with respect to both XNAH and  $\text{Cu}^{2+}$ . The oxidation reaction was found to be independent and parallel to the acid-catalyzed hydration reaction of XNAH. The catalytic role of  $\text{Cu}^{2+}$  for the oxidation of XNAH in the presence of  $\text{O}_2$  was attributed to  $\text{Cu}^{2+}/\text{Cu}^+$  redox cycle by the reactions with XNAH and  $\text{O}_2$ . The second order rate constants of the  $\text{Cu}^{2+}$  oxidation reaction  $k_{\text{Cu}}$  and acid-catalyzed hydration reaction  $k_{\text{H}}$  were strongly dependent on the nature of the substituents in 1-aryl moiety. The slopes of  $\log k_{\text{Cu}}$  vs  $\log k_{\text{H}}$  and  $\log k_{\text{Cu}}$  vs  $\sigma_p$  of the substituents plots were 1.64 and -2.2, respectively. This revealed the greater sensitivity of the oxidation reaction rate to the electron density on the ring nitrogen than the hydration reaction rate. A concerted two-electron transfer route involving XNAH- $\text{Cu}^{2+}$  complex was proposed for mechanism of the oxidation reaction.

### Introduction

The redox couple  $\text{NADH}/\text{NAD}^+$  is one of the most important coenzymes in biological systems. In consequence the chemical reactions of NADH model compounds in enzyme-free systems have been a major interest to chemists.<sup>1</sup> The detailed mechanism of NADH model compounds reduction of organic substances is still in controversy whether the net transfer of hydride from the 4-position of the dihydropyridine ring to the oxidizing agent is a single step process or via multi-step  $e^-$ ,  $\text{H}^+$ ,  $e^-$  mechanism.<sup>2</sup> Meanwhile, it was shown that oxidation of NADH and its analogues by inorganic one-electron oxidants such as ferrocenium cation<sup>3,4</sup> and ferricyanide anion<sup>5-7</sup> proceeds by rate-determining initial one-electron transfer from dihyronicotinamide moiety to the oxidizing agent. The logarithm of the reaction rate constant appeared to vary linearly with  $E^0$  for ferrocenium/ferrocene couples.<sup>4</sup> Divalent metal ions exert large effects on reduction of organic compounds by dihyronicotinamides.<sup>1b,1c</sup> They catalyze the reaction and, sometimes, increase stereoselectivity in the reduction.

In this paper we report oxidation of 1-benzyl- and 1-aryl-substituted-1,4-dihyronicotinamides **1-6** by  $\text{Cu}^{2+}$  in aqueous media. The effect of the nature of the 1-substituents on the oxidation rate was evaluated and correlated with that on the hydration reaction of the dihyronicotinamides.<sup>8</sup> We also show a large effect of oxygen on the kinetics of the oxidation reaction.



- 1**, X =  $\text{C}_6\text{H}_5\text{CH}_2$     **2**, X =  $p\text{-CH}_3\text{OC}_6\text{H}_4$   
**3**, X =  $p\text{-CH}_3\text{C}_6\text{H}_4$     **4**, X =  $\text{C}_6\text{H}_5$   
**5**, X =  $p\text{-ClC}_6\text{H}_4$     **6**, X =  $p\text{-CNC}_6\text{H}_4$

### Experimental

**Materials.** The NADH model compounds 1-benzyl-1,4-dihyronicotinamide(**1**), 1-(*p*-methoxyphenyl)-1,4-dihyronicotinamide(**2**), 1-(*p*-methylphenyl)-1,4-dihyronicotinamide(**3**), 1-phenyl-1,4-dihyronicotinamide(**4**), 1-(*p*-chlorophenyl)-1,4-dihyronicotinamide(**5**) and 1-(*p*-cyanophenyl)-1,4-dihyronicotinamide(**6**) were available from an earlier study.<sup>8</sup> Vacuum dried  $\text{CuCl}_2$ (Junsei) was used as a source of  $\text{Cu}^{2+}$ . Deionized glass-distilled water was used. All other chemicals were readily available from commercial sources.

**Kinetic Studies.** Rate constants for the disappearance of dihyronicotinamides (XNAH) **1-6** were determined at 25 °C with a Spectronic 21 or Beckman DU 8B UV-VIS spectrophotometer with a thermostatted cell holder. The ionic strength of solutions was held constant at 0.1 M by the addition of NaCl. The buffer system was 0.01 M cacodylate. The reaction was made by mixing a solution of XNAH in ethanol with an aqueous  $\text{Cu}^{2+}$  solution at a desired pH (or  $\text{H}^+$  concentration) in a quartz mixing cell. The final solvent composition was 5% EtOH-95%  $\text{H}_2\text{O}$  and the concentration of XNAH was  $1.0 \times 10^{-4}$  M.

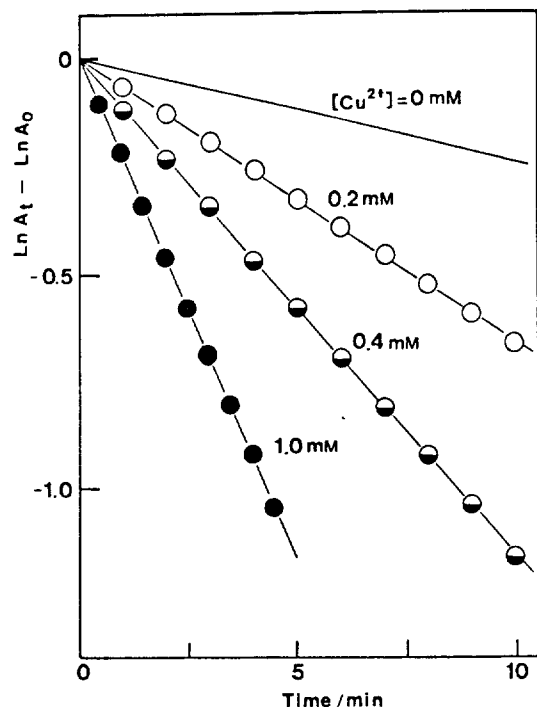


**Figure 1.** Plots of logarithm of absorbance of BNAH at 354 nm against reaction time according to eq. 1 at various concentrations of  $\text{Cu}^{2+}$  shown. The pH of solutions was 5.3.

To investigate an effect of oxygen, the anaerobic kinetic runs were carried out. For removal of oxygen from solutions, nitrogen gas which was purified by passing through  $\text{NH}_4\text{VO}_3/\text{Zn}(\text{Hg})$  was bubbled into a desired reaction mixture without XNAH in a quartz cell with a stopcock for an hour and then 0.01 ml of 0.01 M solution of XNAH in ethanol was added through a Hamilton syringe. The stopcock was immediately closed, the solution was mixed and the reaction was followed spectrophotometrically.

Disappearance of XNAH was followed by observing the decrease in absorbance ( $A$ ) of the solution during the reaction at their characteristic absorption peaks, 340-360 nm region. For dihydronicotinamides **1**, **3** and **5**, of which reaction products do not show appreciable absorption at the measuring wavelength, the pseudo first order rate constant ( $k_\psi$ ) were determined from plots according to equation 1.

$$\ln A_t - \ln A_0 = -k_\psi t \quad (1)$$

For compounds **2**, **4** and **6** whose reaction products have some absorption at the measuring wavelength,  $k_\psi$ 's were determined from the plots of  $\ln(A_t - A_{t+\Delta t})$  against time:<sup>9</sup>

$$\ln(A_t - A_{t+\Delta t}) = -k_\psi t + \ln(1 - e^{-k_\psi \Delta t}) + \text{constant} \quad (2)$$

## Results and Discussion

### Evidences of Oxidation and the Rate Constants.

Figure 1 shows plots of the logarithm of absorbance of 1-benzyl-1,4-dihydronicotinamide (BNAH) **1** at 354 nm against time (eq 1) at various concentration of  $\text{Cu}^{2+}$ . The Figure shows a good linearity, which indicates that the disappearance of BNAH follows pseudo first-order kinetics both in the presence and in the absence of  $\text{Cu}^{2+}$ . It also shows the linear increase of the slope  $k_\psi$ , the pseudo first-order rate constant, with  $[\text{Cu}^{2+}]$ . Such relationships were

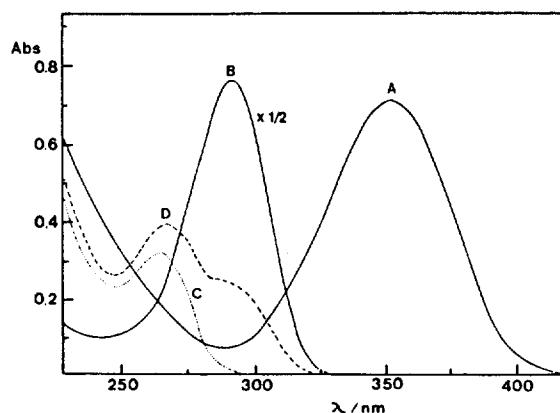


**Figure 2.** UV spectra of BNAH (A), BNAH without  $\text{Cu}^{2+}$  after one day (B), BNAH with  $\text{Cu}^{2+}$  after one day (D) and 1-benzyl-3-carbamoylpyridinium salt (C). For details on conditions, see text.

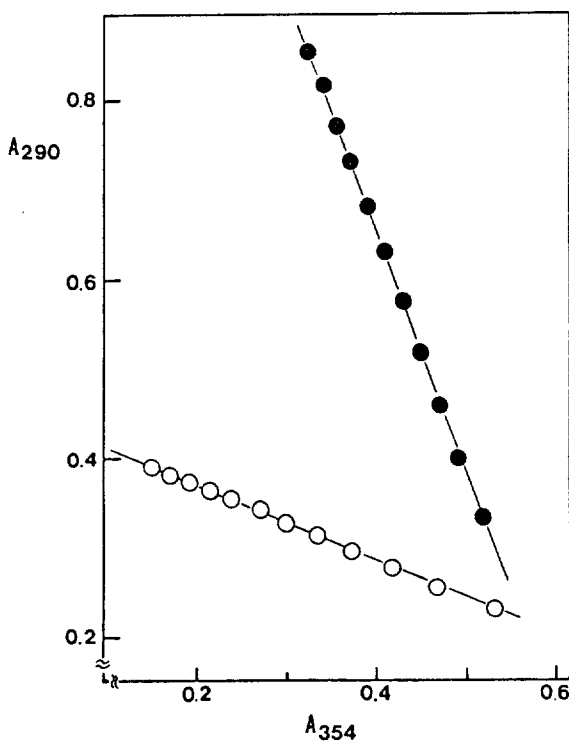


**Figure 3.** The relationships between absorbances at 290 nm and 354 nm of  $1.0 \times 10^{-4}$  M BNAH solutions in the absence of  $\text{Cu}^{2+}$  (●) and in the presence of  $2.0 \times 10^{-4}$  M  $\text{Cu}^{2+}$  (○) at various reaction times. The pH of solutions was 6.0.

also obtained with other XNAH's studied here.

Dihydronicotinamides undergo  $\text{H}^+$  catalyzed hydration reactions.<sup>8</sup> The enhanced rate of disappearance of XNAH in the presence of  $\text{Cu}^{2+}$  can be attributed either to a catalytic effect of the metal ion on the hydration or to other parallel reaction in which  $\text{Cu}^{2+}$  is involved. To clarify this, the UV spectra of the reaction products from BNAH were taken and shown in Figure 2. The A and C represent spectra of BNAH itself and its oxidized product, 1-benzyl-3-carbamoylpyridinium salt, respectively. The spectra B and D were taken after standing BNAH solution in pH 5.9 buffer for a day without  $\text{Cu}^{2+}$  (B) and with  $5.0 \times 10^{-4}$  M  $\text{Cu}^{2+}$  (D). B represents the spectrum of the hydrated product of BNAH, 1-benzyl-6-hydroxy-1,4,5,6-tetrahydronicotinamide.<sup>10</sup> Com-

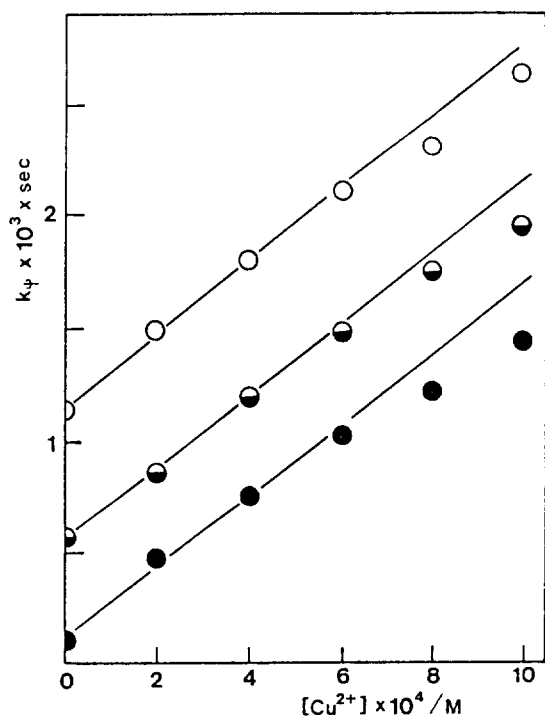


**Figure 4.** The plots of the pseudo first-order rate constant  $k_p$  of 1-(p-methylphenyl)-1,4-dihydronicotinamide **3** as functions of  $[\text{Cu}^{2+}]$ . The concentrations of  $\text{H}^+$  in solutions are  $1.0 \times 10^{-3}$  (○),  $5.0 \times 10^{-4}$  (◐) and  $1.0 \times 10^{-4}$  M (●).

paring the spectrum D with the spectra B and C, it is clear that BNAH undergoes both hydration and oxidation reactions in the presence of  $\text{Cu}^{2+}$ : addition of  $\text{Cu}^{2+}$  to XNAH solutions causes an additional reaction, oxidation of XNAH.

Now the question is whether the cupric ion causes just oxidation of XNAH or it also has any effect on the hydration reaction. Since the hydrated product has the characteristic absorption band at 290 nm, and both BNAH itself and its oxidized product do not have any appreciable absorption at the wavelength, the absorbance at 290 nm reflects only hydration reaction product. Figure 3 shows the relationships between absorbance values at 290 nm and 354 nm for  $1.0 \times 10^{-4}$  M BNAH solutions in the absence and in the presence of 0.2 mM  $\text{Cu}^{2+}$  at pH 6.0 taken at various reaction times. Good linearity between the absorbances values was observed, but the slopes were different. When the cupric ion was absent, the slope was  $-2.67$ : the minus sign reflects that the hydrated product absorbing at 290 nm is formed at the expense of BNAH absorbing at 354 nm, and the value 2.67 is the ratio of the molar absorptivities of the hydrated product and BNAH itself. In the presence of 0.2 mM  $\text{Cu}^{2+}$ , the slope was decreased to  $-0.43$ . This suggests that only 1/6 of the BNAH consumed undergoes hydration reaction and the remaining 5/6 is oxidized. Using the same experimental data, the pseudo first-order rate constants ( $k_p$ 's) for the disappearance of BNAH were calculated to be  $1.56 \times 10^{-4} \text{ sec}^{-1}$  in the absence of  $\text{Cu}^{2+}$  and  $9.44 \times 10^{-4} \text{ sec}^{-1}$  in the presence of 0.2 mM  $\text{Cu}^{2+}$ . The ratio is also 1:6. Therefore the six times increase in the rate constant for the disappearance of BNAH in the presence of 0.2 mM  $\text{Cu}^{2+}$  can be attributed solely to the oxidation of BNAH by  $\text{Cu}^{2+}$ . Thus we can conclude that the presence of  $\text{Cu}^{2+}$  has no noticeable effect on the hydration reaction of BNAH in our experimental condition.

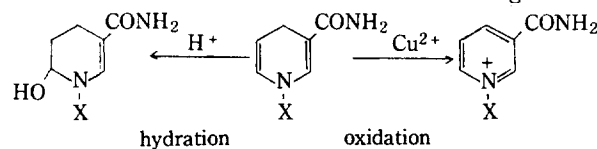
**Table 1.** Second Order Rate Constants of Hydration  $k_H$  and Cupric Ion Oxidation  $k_{\text{Cu}}$  of Dihydronicotinamides at 25°C in 5% Ethanol-95%  $\text{H}_2\text{O}$  of Ionic Strength 0.1 M

Compounds	x	$k_H, \text{M}^{-1}\text{sec}^{-1}$	$k_{\text{Cu}}, \text{M}^{-1}\text{sec}^{-1}$
1	$\text{C}_6\text{H}_5\text{CH}_2$	13.6	3.97
2	$\text{CH}_3\text{OC}_6\text{H}_4$	1.37	2.35
3	$\text{CH}_3\text{C}_6\text{H}_4$	1.14	1.55
4	$\text{C}_6\text{H}_5$	0.665	0.524
5	$\text{ClC}_6\text{H}_4$	0.352	0.195
6	$\text{CNC}_6\text{H}_4$	0.030	0.004

At a given pH or  $\text{H}^+$  concentration, the pseudo first-order rate constant  $k_p$  for the disappearance of XNAH was varied linearly with  $[\text{Cu}^{2+}]$ , except slight negative deviation at high  $[\text{Cu}^{2+}]$ . This relationship was shown for 1-(p-methylphenyl)-1,4-dihydronicotinamide **3** at various HCl concentration in Figure 4. It is evident from this Figure that the second-order rate constant for the oxidation of XNAH by  $\text{Cu}^{2+}$ ,  $k_{\text{Cu}}$ , which is the slope of the  $k_p$  vs  $[\text{Cu}^{2+}]$  plot, is independent of  $[\text{H}^+]$ . The intercept,  $k_p$  at  $[\text{Cu}^{2+}] = 0$ , was shown to be proportional to  $[\text{H}^+]$  and the proportionality constant,  $k_H$ , is the second-order rate constant of the hydration reaction of XNAH catalyzed by  $\text{H}^+$ .<sup>8</sup> From Figure 4 and our discussion in the preceding paragraph, it is evident that the pseudo first-order rate constant for the disappearance of XNAH can be written in terms of two independent parallel reactions.

$$k_p = k_H[\text{H}^+] + k_{\text{Cu}}[\text{Cu}^{2+}] \quad (3)$$

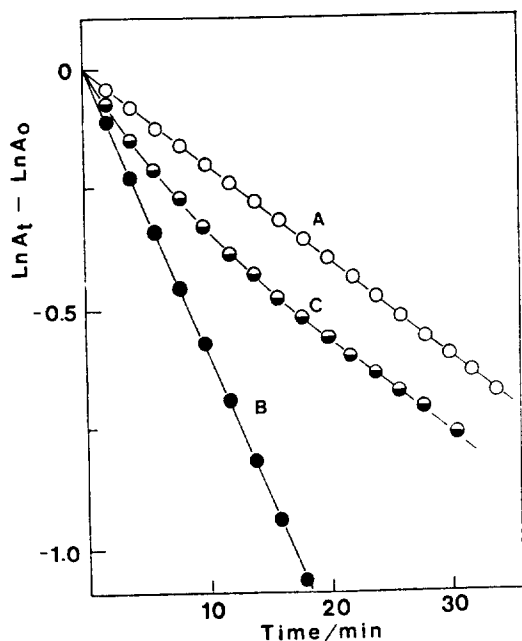
Also, the reactions can be written in the following Scheme:



From the intercept and the slope of the plots of  $k_p$  vs  $[\text{Cu}^{2+}]$  as shown in Figure 4, the second order rate constants,  $k_H$  and  $k_{\text{Cu}}$  were obtained and the results are summarized in Table 1.

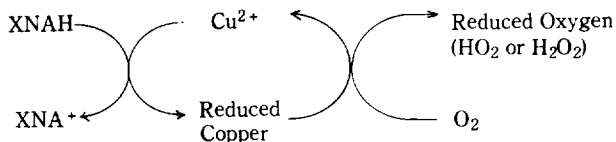
**Effect of Dioxygen-Catalytic Role of  $\text{Cu}^{2+}$  in the Presence of  $\text{O}_2$ .** The fact that the oxidation of XNAH by  $\text{Cu}^{2+}$  is first-order with respect to the initial concentration of  $\text{Cu}^{2+}$  suggests that the concentration of the oxidizing agent remains constant during the reaction. This would be no wonder if  $[\text{Cu}^{2+}] \gg [\text{XNAH}]$ . However, when  $[\text{Cu}^{2+}]$  is not so high compared to  $[\text{XNAH}]$  as in the cases shown in Figures 1 and 4, there should be a route for regeneration of  $\text{Cu}^{2+}$  to maintain the concentration constant. Since we did not add any other oxidizing agent to reoxidize the reduced copper purposely, it seems natural to assume that the  $\text{Cu}^{2+}$  is regenerated by dissolved  $\text{O}_2$  in the reaction system. In fact, it is known that molecular oxygen can be utilized as an oxidant in  $\text{Cu}^{2+}$ -catalyzed oxidation reactions by participation in  $\text{Cu}^{2+}/\text{Cu}^+$  redox cycle.<sup>11,12</sup> The concentration of dissolved  $\text{O}_2$  in aqueous solution at 25°C is calculated to be 0.25 mM.<sup>13</sup> This amount is sufficient to regenerate  $\text{Cu}^{2+}$  from its reduced form produced as a result of oxidation of  $1.0 \times 10^{-4}$  M XNAH.

Figure 5 shows the results of the aerobic and the anaerobic kinetic runs: A is the result obtained in an air-saturated solution without  $\text{Cu}^{2+}$ ; B and C are the data taken in



**Figure 5.** Plots of logarithm of absorbance of  $1.0 \times 10^{-4}$  M BNAH solutions at 354 nm against reaction time according to eq 1. A is the result taken in an air saturated solution without  $\text{Cu}^{2+}$ . B and C represent data from air saturated and  $\text{N}_2$  purged solutions, respectively, containing  $1.0 \times 10^{-4}$  M  $\text{Cu}^{2+}$ . The pH of solutions was adjusted to 5.9, and the final solvent composition was 1% aqueous ethanol.

air-saturated and deaerated solutions with  $1.0 \times 10^{-4}$  M  $\text{Cu}^{2+}$ , respectively. In contrast to the excellent linearity observed in A and B, C deviates considerably from the pseudo first-order rate equation. The tangent of plot C, which is the apparent rate constant  $k_\psi$ , is close to the slope of B at the initial stage of the reaction. But it approaches to that of A as the reaction proceeds. The diminution of  $\text{Cu}^{2+}$  with the progress of the reaction can account for this behavior, since  $\text{Cu}^{2+}$  cannot be regenerated in the absence of oxygen. Alternatively, this result can be regarded as an evidence that  $\text{Cu}^{2+}$  plays a catalytic role on the oxidation of XNAH in the presence of dioxygen. The overall reaction can be expressed in the following cyclic Scheme:



**Effect of Substituents on Oxidation Rate and Reaction Mechanism.** The data in Table 1 show strong dependence of both  $k_H$  and  $k_{\text{Cu}}$  on the nature of the substituent in 1-aryl moiety of XNAH. Figure 6 presents the plots of  $\log k_{\text{Cu}}$  against  $\log k_H$  and  $\sigma_p$  constants of the substituents in 1-aryl groups. The good linear relationships between these values are evident. The Hammett relationship between  $k_{\text{Cu}}$  and  $k_H$  can be expressed as eq 4 except  $X = \text{CNC}_6\text{H}_4$ .

$$\log k_{\text{Cu}} = 1.64 \log k_H + 0.079 \quad (r=0.999) \quad (4)$$

Also, the correlation between  $\log k_{\text{Cu}}$  and  $\sigma_p$  obeyed the following form except  $X = \text{C}_6\text{H}_4\text{CH}_2$ .

$$\log k_{\text{Cu}} = -2.2 \sigma_p - 0.22 \quad (r=0.996) \quad (5)$$

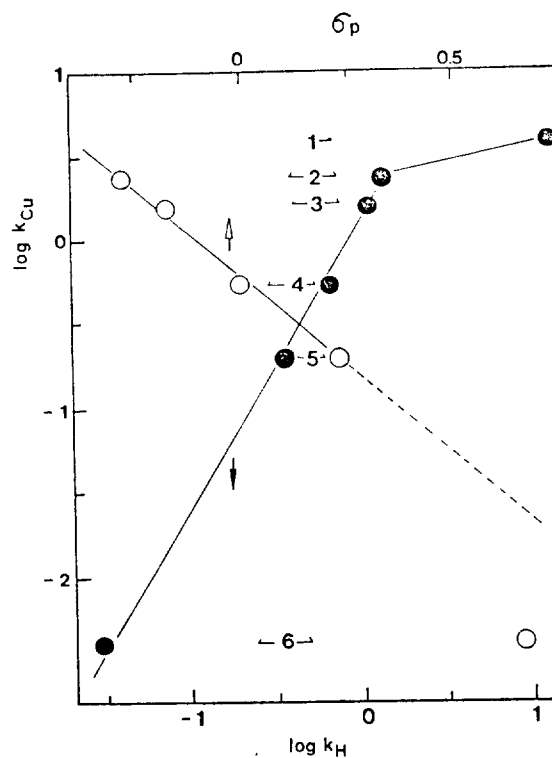


**Figure 6.** Hammett type plots of the second order  $\text{Cu}^{2+}$  oxidation rate constants of dihydropyridinamides against hydration rate constants ( $\bullet$ ) and  $\sigma_p$  of substituents in 1-aryl moiety ( $\circ$ ).

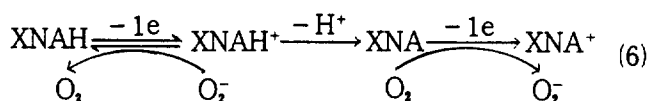
It is obvious from these results that the  $\text{Cu}^{2+}$  oxidation rate is more sensitive to the electron density on the ring nitrogen than the hydration reaction rate.

The  $\text{Cu}^{2+}$  oxidation rate constants  $k_{\text{Cu}}$  obtained in this investigation are 2-4 times greater than the ferricyanide oxidation rate constants for the same XNAH's.<sup>7</sup> This is quite unusual in view of the kinetic-thermodynamic correlation when one considers the difference in the standard redox potentials  $E^0$  of  $\text{Cu}^{2+}/\text{Cu}^+$  0.153 V and  $\text{Fe}(\text{CN})_6^{-3}/\text{Fe}(\text{CN})_6^{-4}$  0.45 V.<sup>14</sup> One of the possible explanations for this is hydride transfer mechanism for cupric ion oxidation, while the ferricyanide oxidation involves the rate determining electron transfer step.<sup>7</sup> However, this is unlikely in the light of hydride chemistry.

An alternative explanation is involvement of complexation between XNAH and  $\text{Cu}^{2+}$ . This could reduce the energy barrier for rate determining electron transfer step and accelerate the reaction. The complex formation between XNAH and metal ions accounted for the catalytic effect of the ions in XNAH reduction of organic compounds in organic media.<sup>15,16</sup> The formation of reactive complex was also reported in ferric ion oxidation of NADH.<sup>17,18</sup> We attempted to obtain an evidence of the XNAH- $\text{Cu}^{2+}$  complex formation, but failed presumably due to small complex formation constant (*vide infra*). The first-order kinetics for the disappearance of XNAH in both XNAH and  $\text{Cu}^{2+}$  implies that only very small fractions of XNAH and  $\text{Cu}^{2+}$  are complexed, if any, in our experimental condition. Moreover the independence of  $k_H$  on  $[\text{Cu}^{2+}]$  supports this view: The hydration reaction of XNAH involves rate determining protonation step, and the step is expected to be inhibited by XNAH- $\text{Cu}^{2+}$  complex formation due to electrostatic effect. This argument was

supported from studies on the effect of metal ions on the hydration reaction in non-aqueous media.<sup>19</sup> The apparent first-order rate constant  $k_{\text{app}}$  is expected to decrease as the fraction of the complexed XNAH increases at higher concentration of  $\text{Cu}^{2+}$ .<sup>20</sup> The negative deviation from linearity in  $k_{\text{app}}$  vs  $[\text{Cu}^{2+}]$  plots at high concentration of  $\text{Cu}^{2+}$  (Figure 4) seems to reveal this. Thus the deviation can be taken as an evidence of weak XNAH- $\text{Cu}^{2+}$  complexation.<sup>21</sup>

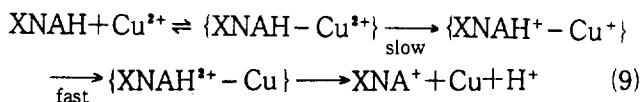
It is of interest to note that  $\text{O}_2$  enhances the  $\text{Cu}^{2+}$  oxidation rate (possibly by oxidation of reduced copper to  $\text{Cu}^{2+}$ ), whereas it inhibits the ferricyanide oxidation of XNAH.<sup>7</sup> The latter observation was attributed to the regeneration of XNAH from  $\text{XNAH}^+$  by reaction with  $\text{O}_2^-$  which is formed from the reaction between XNA and  $\text{O}_2$ . The  $\text{XNAH}^+$  and XNA are reaction intermediates and are formed by initial one-electron transfer and following not-rate determining steps.



The oxidation of XNAH to  $\text{XNA}^+$  is an overall two-electron process. Also  $\text{Cu}^{2+}$  can be reduced by two electrons to Cu as well as by one electron to  $\text{Cu}^+$ . Therefore the  $\text{Cu}^{2+}$  oxidation of XNAH can proceed via one-electron transfer reaction as shown in eq 7 (a concerted or consecutive process) or via a two electron route in eq 8: The former requires two  $\text{Cu}^{2+}$  per one molecule of XNAH, while the latter mechanism involves only one  $\text{Cu}^{2+}$ .



In the first mechanism, the possibility of a concerted process can be ruled out since the reaction was observed to be first order in  $\text{Cu}^{2+}$ . The consecutive two one-electron process in the first mechanism which is similar to the mechanism of ferricyanide oxidation of XNAH,<sup>7</sup> is less likely as we could not observe the inhibitory effect of  $\text{O}_2$  expected from reaction 6. The second mechanism eq 8 does not contradict with our experimental findings. However this mechanism does not necessarily imply one step two-electron transfer from XNAH to  $\text{Cu}^{2+}$ . It only suggests that the transfer of the second electron to  $\text{Cu}^+$  is very fast and completed before break-off of  $\text{XNAH}^+ \cdot \text{Cu}^+$ .



The resultant Cu might undergo auto redox reaction with  $\text{Cu}^{2+}$  to produce  $\text{Cu}^+$  which is oxidized to  $\text{Cu}^{2+}$  by  $\text{O}_2$ . The superoxide  $\text{O}_2^-$  would react with  $\text{H}^+$  to form  $\text{HO}_2$  and  $\text{H}_2\text{O}_2$  by further reactions.

## Conclusions

We have demonstrated that XNAH is oxidized by  $\text{Cu}^{2+}$  in aqueous solution. The reaction is first order with respect to both XNAH and  $\text{Cu}^{2+}$ . The oxidation reaction is independent and parallel to the acid-catalyzed hydration reaction of XNAH. The oxidation and hydration reaction rates depend strongly on the electron-withdrawing characteristics of substituents in 1-aryl moiety. The Hammett type plots of  $\log k_{\text{Cu}}$

against  $\log k_{\text{H}}$  and  $\sigma_{\text{p}}$  yielded good linearity with slopes 1.64 and -2.2, respectively. This indicates greater sensitivity of the  $\text{Cu}^{2+}$  oxidation reaction rate of XNAH to the electron density on the ring nitrogen and reveals electron transfer process in the rate determining step of the oxidation reaction. In the presence of dioxygen,  $\text{Cu}^{2+}$  behaves as a catalyst for the oxidation of XNAH. Though the detailed mechanism for the oxidation is not fully elucidated at this point, a concerted two-electron transfer mechanism involving XNAH- $\text{Cu}^{2+}$  complex was found to be consistent with our experimental observations.

**Acknowledgement.** This work was supported by the Basic Science Research Institute Program of Ministry of Education of the Republic of Korea, 1987.

## References

- (a) D. M. Stout and A. I. Meyers, *Chem. Rev.*, **82**, 223 (1982); (b) Y. Inouye, J. Oda and B. Bada, in "Asymmetric Synthesis", J. D. Morrison Ed., Academic Press, New York, 1983, Vol. 2, pp. 91-124; (c) S. Yasui and A. Ohno, *Bioorg. Chem.*, **14**, 70 (1986).
- For this, see: (a) M. F. Powell and T. C. Bruice, *J. Am. Chem. Soc.*, **105**, 1014 (1983); (b) S. Fukuzumi, N. Nishizawa and T. Tanaka, *J. Chem. Soc. Perkin Trans. II*, 371 (1985).
- B. W. Carlson and L. L. Miller, *J. Am. Chem. Soc.*, **105**, 7453 (1983).
- B. W. Carlson, L. L. Miller, P. Neta and J. Grodkowski, *J. Am. Chem. Soc.*, **106**, 7233 (1984).
- T. Okamoto, A. Ohno and O. Shinzaburo, *Bull. Chem. Soc. Jpn.*, **53**, 330 (1980).
- F. Pavlikova-Raclava and J. Kuthan, *Coll. Czech. Chem. Commun.*, **48**, 1408 (1983).
- M. F. Powell, J. C. Wu and T. C. Bruice, *J. Am. Chem. Soc.*, **106**, 3850 (1984); A. Sinha and J. C. Bruice, *J. Am. Chem. Soc.*, **106**, 7291 (1984).
- K. K. Park, J. G. Yoo and J. W. Park, *Bull. Korean Chem. Soc.*, **8**, 348 (1987).
- J. W. Moore and R. G. Pearson, "Kinetics and Mechanism" 3rd, Ed., Wiley, New York, 1984, pp. 70-74.
- C. C. Johnston, J. L. Gardner, C. H. Suelter and D. E. Metzler, *Biochemistry*, **2**, 689 (1963).
- F. A. Cotton and G. Wilkinson, in "Advanced Inorganic Chemistry", 4th Ed., Wiley, New York, 1980, p. 490 and 820.
- M. J. Harris, A. Herp and W. Pigman, *J. Am. Chem. Soc.*, **94**, 7570 (1972).
- The Henry's law constant of  $\text{O}_2$  in water at 25°C is  $4.4 \times 10^9$  Pa. This gives the concentration of the dissolved  $\text{O}_2$  under atmospheric pressure of  $P_{\text{O}_2}$  of  $2 \times 10^4$  Pa (0.2 atm) as 0.25 mM.
- CRC Handbook of Chemistry and Physics, 60th Ed., p. D-155.
- S. Fukuzumi, Y. Kondo and T. Tanaka, *Chem. Lett.*, 485 (1985).
- S. Fukuzumi, S. Koumitsu, K. Hironaka and T. Tanaka, *J. Am. Chem. Soc.*, **109**, 305 (1987).
- M. Gutman, R. Margalit and A. Schejter, *Biochemistry*, **7**, 2778 (1968).
- M. Gutman and M. Eisenbach, *Biochemistry*, **12**, 2314 (1973).

19. To be published.

20. The oxidation rate is given by:

$$\begin{aligned} \text{Rate} &= k[\text{XNAH}\cdot\text{Cu}^{2+}] \\ &= kK(1-f_{\text{XNAH}})(1-f_{\text{XNAH}}[\text{XNAH}]_t/[\text{Cu}^{2+}]_t) \times [\text{XNAH}]_t \\ &\quad [\text{Cu}^{2+}]_t \\ &= k_{\text{Cu}}[\text{XNAH}]_t [\text{Cu}^{2+}]_t \end{aligned}$$

Thus the apparent second order oxidation rate constant  $k_{\text{Cu}}$  decreases as the complexed fraction of XNAH,

$f_{\text{XNAH}}$  increases for a given complex formation constant  $K$ . The  $k$  is the intrinsic electron transfer rate constant of the complex and  $k_{\text{Cu}}$  becomes  $kK$  as  $f_{\text{XNAH}} \rightarrow 0$ .

21. At condition of  $[\text{Cu}^{2+}] \gg [\text{XNAH}]$ , the concentration of XNAH-Cu<sup>2+</sup> complex is proportional to total concentration of XNAH by  $[\text{XNAH}\cdot\text{Cu}^{2+}] = K[\text{Cu}^{2+}][\text{XNAH}]_t / (1 + K[\text{Cu}^{2+}])$ . Thus the first order kinetics in XNAH expressed in eq. 1 is still valid.

## Four Crystal Structures of Dehydrated $Ag^+$ and $Tl^+$ Exchanged Zeolite A, $Ag_{12-x}Tl_xA$ , $x = 2, 3, 4$ , and 5

Duk Soo Kim, Seong Hwan Song\*, and Yang Kim\*

Department of Chemistry, Cheju National University, Cheju 690-756

\*Department of Chemistry, Pusan National University, Pusan 609-745. Received April 15, 1988

Four crystal structures of dehydrated  $Ag(I)$  and  $Tl(I)$  exchanged zeolite A,  $Ag_{12-x}Tl_xA$ ,  $x = 2, 3, 4$ , and 5, have been determined by single-crystal x-ray diffraction techniques. Their structures were solved and refined in the cubic space group  $Pm\bar{3}m$  at 21(1) °C. All crystals were ion exchanged in flowing streams of mixed  $AgNO_3$  and  $TlNO_3$  aqueous solution, followed by dehydration at 350 °C and  $2 \times 10^{-6}$  Torr for 2 days. In all of these structures, one-sixth of the sodalite units contain octahedral hexasilver clusters at their centers and eight  $Ag^+$  ions are found on threefold axes, each nearly at the center of a 6-oxygen ring. The hexasilver cluster is stabilized by coordination to eight  $Ag^+$  ions. The  $Ag$ - $Ag$  distance in the cluster, ca. 2.92 Å, is near the 2.89 Å bond length in silver metal. The remaining five-sixths of the sodalite units are empty of silver species. The first three  $Tl^+$  ions per unit cell preferentially associate with 8-oxygen rings, and additional  $Tl^+$  ions, if present, are found on threefold axes in the large cavity.

### Introduction

The properties of zeolites are sensitive to their cationic contents. A knowledge of the siting of these cations within a zeolite framework can provide a structural basis for understanding these properties. Thus far, the structures of  $Ag^+$ <sup>1,2</sup>,  $K^+$ <sup>3,4</sup>,  $Rb^+$ <sup>5</sup>,  $Cs^+$ <sup>6</sup>,  $Tl^+$ <sup>7</sup>,  $Mn(II)$ <sup>8,9</sup>,  $Co(II)$ <sup>9,12</sup>,  $Ni(II)$ <sup>9</sup>,  $Zn(II)$ <sup>9,13</sup>,  $Ca^{2+}$ <sup>14</sup>, and  $Eu(II)$ <sup>15</sup> exchanged zeolite A<sup>16</sup> have been determined crystallographically.

Recently several crystal structures of fully  $Ag^+$ -exchanged zeolite A were determined.<sup>17</sup> Fully dehydrated  $Ag_{12}A$  contains silver atoms, probably as hexasilver molecules centered within some of its sodalite cavities. Hexasilver is stabilized by coordination to eight  $Ag^+$  ions very near the centers of the 6-oxygen rings on threefold axes.<sup>2,17</sup> Hermer-schmidt and Haul identified  $Ag_6^{n+}$  ( $n < 6$ ) clusters in the soda-

lite cavity of dehydrated  $Ag^+$ -exchanged zeolite A using epr spectroscopy.<sup>18</sup> Their results were verified by Grobet and Schoonheydt<sup>19</sup> and reverified by the careful work of Morton and Preston who did epr measurements on isotropically pure samples of  $Ag_{12}A$ <sup>20</sup>.

The present study has been initiated to investigate the cation positions in the crystal structures of variously  $Ag^+$  and  $Tl^+$  exchanged zeolite A. It would be interesting to learn how different numbers of exchanged  $Tl^+$  ions arrange themselves in the zeolite framework. Furthermore, because of the high scattering powers of  $Tl^+$  and  $Ag^+$ , precise and reliable crystallographic determinations should be easy to achieve. The present work is preliminary to later studies of the crystal structure of  $Ag_{12-x}Tl_xA$  treated with  $H_2$  or other guest molecules.

Table 1. A Summary of Experimental Results

Crystal	Zeolite Cation Composition	Ion Exchange		Temp. (°C)	Dehydration		Unit Cell Constant(Å)	Number of <sup>a</sup>		
		Mole ratio ( $AgNO_3:TlNO_3$ )	Period		Temp.	Pressure (Torr.)		Observed Reflections	$R_1$	$R_2$
1	$Ag_{10}Tl_2A$	5:1	2 days	350	2	$2 \times 10^{-6}$	12.300(2) <sup>b</sup>	302	0.054	0.057
2	$Ag_9Tl_3A$	1.9:1	2 days	350	2	$2 \times 10^{-6}$	12.243(2)	256	0.070	0.070
3	$Ag_8Tl_4A$	1:1	2 days	350	2	$2 \times 10^{-6}$	12.281(1)	377	0.067	0.067
4	$Ag_7Tl_5A$	1:5	2 days	350	2	$2 \times 10^{-6}$	12.263(1)	323	0.055	0.063

<sup>a</sup>Only those reflections for which  $I > 3\sigma(I)$  were considered observed. <sup>b</sup>The number in parentheses is the esd in the units of the least significant digit given.